Am Min Ms 5407 Revision 1

Geobarometry from host-inclusion systems: the role of elastic relaxation

Ross J. Angel[1], Mattia L. Mazzucchelli[2], Matteo Alvaro[1], Paolo Nimis[1], Fabrizio Nestola[1]

[1]Department of Geosciences, University of Padua, Via G. Gradenigo 6, Padua, 35131, Italy
[2]Department of Earth and Environmental Sciences, University of Pavia, Via A. Ferrata, 1, Pavia, 27100, Italy.

Correspondence e-mail: rossjohnangel@gmail.com

Submitted to: *American Mineralogist, Letters*

Version of 08/07/2014

Always consult and cite the final, published document. See http://www.minsocam.org or GeoscienceWorld

Abstract

Minerals trapped as inclusions within other host minerals can develop residual stresses on exhumation as a result of the differences between the thermo-elastic properties of the host and inclusion phases. The determination of possible entrapment pressures and temperatures from this residual stress requires the mutual elastic relaxation of the host and inclusion to be determined. Previous estimates of this relaxation have relied on the assumption of linear elasticity theory. We present a new formulation of the problem that avoids this assumption. We show that for soft inclusions such as quartz in relatively stiff host materials such as garnet, the previous analysis yields entrapment pressures in error by the order of 0.1 GPa. The error is larger for hosts that have smaller shear moduli than garnet.

Introduction

Minerals trapped as inclusions within other host minerals can develop residual stresses on exhumation as a result of the differences between the thermo-elastic properties of the host and inclusion phases (e.g. Fig 3. in Howell et al. 2010). Measurement of the residual stress in the inclusions can, in combination with the equations of state (EoS) of the two phases, be used to infer the pressures and temperatures of entrapment if no plastic deformation has occurred (e.g. Zhang 1998; Izraeli et al. 1999; Guiraud and Powell 2006; Howell et al. 2012; Kohn 2014; Kouketsu et al. 2014). The key concept is that when the inclusion was trapped, the host and inclusion had the same P and T, and the inclusion fitted perfectly within the cavity in the host (Fig. 1a), so there were no stress gradients across the host and inclusion.

Consider a soft inclusion in a relatively stiff host recovered from metamorphic conditions to room conditions. The volume change of the host will be less than that expected for a free

Always consult and cite the final, published document. See http://www.minsocam.org or GeoscienceWorld

crystal of the inclusion phase. The inclusion phase is therefore compressed to a smaller volume than expected for the final external P and T and is therefore under pressure. The volume change of the host can be calculated from its EoS. The pressure P_I^* in the inclusion is then calculated from this final host volume and the temperature, using the EoS of the inclusion. At this point, the host is under the external pressure, $P_{H,end}$, but the inclusion is under a stress P_I^* (Fig. 1b). This is a physically unstable “virtual’’ state because there is a difference in radial stress at the host/inclusion wall that will force the wall outwards because $P_I^* > P_{H,end}$. This expansion leads to compression of the host and thus an increase in the radial stress in the host adjacent to the inclusion, and a relaxation of the pressure inside the inclusion, $\Delta P_{I,relax}$. The resulting expansion of the inclusion continues until the radial stress in the inclusion matches that in the host adjacent to the inclusion (Fig. 1c) with a stress gradient in the host that decreases to the external stress at the outside surface of the host (Goodier 1933; Eshelby 1957; Fig. 1c).

The final observed inclusion pressure $P_{I,end}$ is therefore comprised of two parts,

$$P_{I,end} = P_I^* + \Delta P_{I,relax}$$

Since P_I^* can be calculated from the EoS of the two phases, the problem of estimating entrapment conditions from observed inclusion pressures lies in the calculation of the change in pressure upon relaxation. Previous calculations (e.g. Zhang 1998; Izraeli et al. 1999; Guiraud and Powell 2006; Howell et al. 2012; Kohn 2014; Kouketsu et al. 2014) all rely on an estimate of the relaxation as $\Delta P_{I,relax} = \frac{-3K_I\left(P_{I,end} - P_{H,end}\right)}{4G_H}$. The derivation of this formula (Zhang 1998) relies on several assumptions including that the inclusion is small and spherical and that both phases are elastically isotropic. We will retain these assumptions. But Zhang’s

Always consult and cite the final, published document. See http://www.minsocam.org or GeoscienceWorld

(1998) derivation also relied on the assumptions of linear elasticity; that the elastic properties of the host and the inclusion do not change with *P* or *T*. This last condition is clearly not valid for changes in pressure and temperature that are geologically relevant. Here we derive a new expression for the relaxation $\Delta P_{I,relax}$ by an approach that does *not* require this assumption.

Methodology

We first address the 'forward problem' of calculating the final pressure on the inclusion at $P_{H,end}$ and T_{end}, following entrapment at conditions P_{trap} and T_{trap}. Elastic deformation is reversible by definition. Therefore the stress and strain in the system of host and inclusion are independent of the path taken from entrapment to the final state, and the final inclusion pressure $P_{I,end}$ is the same for any *P*-*T* path. Instead of performing calculations for a *P*-*T* path of isothermal decompression followed by cooling (e.g. Zhang 1998; Howell et al. 2010), we consider a simultaneous reduction of pressure and temperature from entrapment conditions along a path on which the fractional volume changes of the host and inclusion are the same. Such a path is known as an 'isomeke' (Adams et al. 1975), whose instantaneous slope is determined by the ratio of the differences in volume thermal expansion coefficients and compressibilities of the two phases, $(\partial P/\partial T)_{isomeke} = \Delta\alpha/\Delta\beta$ (Rosenfeld and Chase 1961). Isomekes are therefore curved lines in *P*-*T* space (Fig. 2) that can be calculated directly from the EoS of the host and the inclusion, without any restrictions on the form of the EoS, and especially no requirement for the elastic properties of either phase to be constant.

We now consider the cooling of the system along the isomeke from entrapment at P_{trap} and T_{trap} to the final temperature T_{end}. The key point is that, because we have moved the system along an isomeke from the initial state, the stress in both the inclusion and the host is uniform and equal to the external pressure, which we denote P_{foot} (Fig 2) to indicate we are at the *foot* of the isomeke. So we can now apply the analysis of Goodier (1933) to the isothermal

Always consult and cite the final, published document. See http://www.minsocam.org or GeoscienceWorld

decompression of the host from P_{foot} to $P_{H,end}$. Goodier (1933) showed that, starting from a system in uniform stress and strain, the final stress state is determined solely by the elastic properties of the system and the volume strain ε_H applied at infinity to the host (at constant temperature). Under these conditions the volume strain of the inclusion after the application of the strain ε_H to the host is uniform and constant and given exactly by $\varepsilon_H(1-K_{21})$, using the notation of Torquato (2002). The parameter K_{21} is an elastic interaction parameter whose value is dependent on the elastic properties of both the host and inclusion: $K_{21} = \dfrac{K_I - K_H}{K_I + \frac{4}{3}G_H}$.

The volume strain of the inclusion is thus comprised of two parts, $\varepsilon_H(1-K_{21}) = \varepsilon_H - \varepsilon_H K_{21}$. The first part ε_H is the fractional volume change of the inclusion equal to that of the host, which arises from the decompression of the host from P_{foot} on the original isomeke to $P_{H,end}$ and gives rise to the pressure P_I^* on the inclusion (Fig. 1b, 2). Therefore the second term in the inclusion strain, $-\varepsilon_H K_{21}$ corresponds to the volume relaxation, which results in the relaxation in pressure of $\Delta P_{I,relax}$ (Fig. 1c, 2). Since the pressure variation of all terms in K_{21} will be similar, it is reasonable to assume that K_{21} remains constant over the small pressure interval (typically < 1 GPa) of $\Delta P_{I,relax}$. That is the *only* approximation that is made in our derivation because $\Delta P_{I,relax}$ is then calculated from the volume change $-\varepsilon_H K_{21}$ and the full EoS of the inclusion.

This new approach via the isomeke provides a way to calculate final inclusion pressures arising from the entrapment conditions, for any type of EoS. It also allows the calculation of entrapment conditions from a measured residual pressure on an inclusion ($P_{I,end}$), as follows. First, the value of P_{foot} at T_{end} is found that will produce the observed pressure $P_{I,end}$. The

Always consult and cite the final, published document. See http://www.minsocam.org or GeoscienceWorld

isomeke passing through P_{foot}, T_{end} is then calculated from the EoS parameters of the host and inclusion, and this line represents possible entrapment conditions. Both the forward and reverse calculations can be performed with any common choice of *P*-*V*-*T* EoS, including that of Holland and Powell (2011), and both are implemented in the EosFit7c program (Angel et al. 2014).

Implications

By considering the elastic problem of a host-inclusion system in terms of an initial *P*-*T* path along an isomeke, we have provided a solution to the relaxation problem that is firmly based in conventional elasticity theory (Goodier 1933). We now see that the 'thermodynamic' part, P_I^*, of the final inclusion pressure effectively arises solely from the isothermal decompression of the host from P_{foot} to $P_{H,end}$. More importantly, the relaxation in pressure $\Delta P_{I,relax}$ does not arise from the entire decompression from entrapment, but only from the isothermal pressure change from P_{foot} on the isomeke to $P_{H,end}$. As we show in the Appendix, this means that the relaxation term of Zhang (1998) can be obtained from our solution by assuming constant elastic properties of the host and inclusion over the isothermal decompression from P_{foot}. This explains why the method of Zhang (1998), which was derived by explicitly assuming linear elasticity for all *P* and *T*, may provide good estimates of $P_{I,end}$, especially when the final state is at room conditions. For example, for a quartz inclusion originally entrapped in a garnet at 0.7 GPa and 380^{o}C (Parkinson 2000), the Zhang (1998) method yields a $P_{I,end}$ =0.45 GPa, only 0.01 GPa higher than the correct solution (Fig. 3). However, as the difference between P_{foot} and $P_{H,end}$ increases, the accuracy of the Zhang (1998) model decreases. Thus for a quartz trapped further along the pro-grade path at ~1.7 GPa and ~600^{o}C, P_{foot} = 2.0 GPa (Fig. 3) and the final inclusion pressure will be 1.06 GPa, whereas the Zhang (1998) model overestimates this by 0.08 GPa. The same magnitude of

Always consult and cite the final, published document. See http://www.minsocam.org or GeoscienceWorld

This is a preprint, the final version is subject to change, of the American Mineralogist (MSA)
Cite as Authors (Year) Title. American Mineralogist, in press.
(DOI will not work until issue is live.) DOI: http://dx.doi.org/10.2138/am-2014-5047

error occurs when the entrapment conditions are calculated from a final observed inclusion pressure, but with opposite sign; the Zhang (1998) model underestimates the entrapment pressure at a given temperature. Because the shear modulus of the host appears in the denominator of the equations for relaxation, the error will be larger for host materials with smaller shear moduli than garnet. For stiffer host materials such as diamond, the errors are smaller.

The same trend of increasing error with the magnitude of ($P_{foot} - P_{H,end}$) can be seen in calculations of $P_{I,end}$ along the prograde metamorphic evolution following entrapment of the inclusion. Take the example of the quartz trapped in the cores of the garnets in the Kulet whiteschist (Parkinson 2000) and illustrated in Figure 3. Pro-grade compression from entrapment at 0.7 GPa and 380°C to peak conditions of around 3.5 GPa and 780 °C leads to a P_{foot} = 0.52 GPa and $P_I^* = 1.21\text{GPa}$. Because P_I^* is less than the external pressure, the relaxation acts to increase the pressure on the inclusion. The exact solution yields $\Delta P_{I,relax}$ = +0.51 GPa, and a final inclusion pressure of 1.72 GPa. If the Zhang (1998) expression is used, but with the values of K_I = 51.3 GPa, G_H ~ 88 GPa appropriate for garnet at the peak conditions, one over-estimates the relaxation and the peak inclusion pressure by 0.2 GPa. Interestingly, if one naively uses the exact Zhang (1998) formulation with the clearly inappropriate elastic parameters for room pressure, this overestimate of $\Delta P_{I,relax}$ is almost exactly cancelled out by the value of K_I = 37.1 GPa. Such cancellation cannot be relied upon to occur in all cases!

We caution that, like previous analyses, this approach only considers elastic behaviour and assumes that no plastic deformation occurs. All of these calculations also assume that both the host and the inclusion are elastically isotropic, that the inclusion is isolated elastically

Always consult and cite the final, published document. See http://www.minsocam.org or GeoscienceWorld

from any other inclusion or surface, and that the inclusion is spherical. Isolated inclusions containing gas, melt or fluid in glass hosts meet these requirements. While hosts such as garnet are approximately elastically isotropic (e.g. Sinogeikin and Bass 2000) common inclusion minerals such as quartz are not. As a consequence of this elastic anisotropy one can calculate that the deviatoric stress in typical quartz inclusions in metamorphic garnets will be of the order of 20-40% of the average stress. Further, the volume change of the inclusion also depends on its shape, even in an elastically isotropic host (e.g. Eshelby 1957; Burnley and Davis 2004). Thus the current analysis should not be considered to represent an exact solution for real host/inclusion systems, but instead to approximate their average response to changes in P and T, upon which the anisotropic response can be considered subsequently as a perturbation. But this is only true if measurements of the inclusion yield the true average stress, to be used as $P_{I,end}$. Techniques such as *in-situ* X-ray diffraction of the inclusion do reveal both the anisotropic stress state and its homogeneity (Nestola et al. 2011). But single measurements of the Raman band positions from quartz inclusions (e.g. Kohn 2014; Kouketsu et al. 2014), however, may not reveal the average stress state because of the sensitivity of Raman band positions to anisotropic stresses (Briggs and Ramdas 1977).

Acknowledgements

This analysis was financially supported by an ERC Starting Grant 307322 to F. Nestola (project INDIMEDEA). We thank Christian Chopin, Jerome Fortin, Evangelos Moulas and an anonymous reviewer for their extremely helpful suggestions for the presentation.

Always consult and cite the final, published document. See http://www.minsocam.org or GeoscienceWorld

References

.

Adams, H.G., Cohen, L.H., and Rosenfeld, J.L. (1975) Solid inclusion piezothermometry I: comparison dilatometry. American Mineralogist, 60, 574-583.

Angel, R.J., Gonzalez-Platas, J., and Alvaro, M. (2014) EosFit7c and a Fortran module (library) for equation of state calculations. Zeitschrift fuer Kristallographie, 229, 405-419.

Angel, R.J., Allan, D.R., Miletich, R., and Finger, L.W. (1997) The use of quartz as an internal pressure standard in high-pressure crystallography. Journal of Applied Crystallography, 30, 461-466.

Briggs, R.J., and Ramdas, A.K. (1977) Piezospectroscopy of the Raman spectrum of α-quartz. Physical Review B, 16, 3815-3826.

Burnley, P.C., and Davis, M.K. (2004) Volume changes in fluid inclsuions produced by heating and pressurisation: an assessment by finite element modelling. Canadian Mineralogist, 42, 1369-1382.

Eshelby, J.D. (1957) The determination of the elastic field of an ellipsoidal inclusion, and related problems. Proceedings of the Royal Society of London. Series A. Mathematical and Physical Sciences, 241, 376-396.

Goodier, J.N. (1933) Concentration of stress around spherical and cylindrical inclusions and flaws. Transactions of the American Society of Mechanical Engineers, 39-44.

Guiraud, M., and Powell, R. (2006) *P–V–T* relationships and mineral equilibria in inclusions in minerals. Earth and Planetary Science Letters, 244, 683-694.

Holland, T.J.B., and Powell, R. (2011) An improved and extended internally consistent thermodynamic dataset for phases of petrological interest, involving a new equation of state for solids. Journal of Metamorphic Geology, 29, 333-383.

Howell, D., Wood, I.G., Nestola, F., Nimis, P., and Nasdala, L. (2012) Inclusions under remnant pressure in diamond: a multi-technique approach. European Journal of Mineralogy, 24, 563-573.

Howell, D., Wood, I.G., Dobson, D.P., Jones, A.P., Nasdala, L., and Harris, J.W. (2010) Quantifying strain birefringence halos around inclusions in diamond. Contrib Mineral Petrol, 160, 705-717.

Izraeli, E., Harris, J., and Navon, O. (1999) Raman barometry of diamond formation. Earth and Planetary Science Letters, 173, 351-360.

Always consult and cite the final, published document. See http://www.minsocam.org or GeoscienceWorld

Kohn, M.J. (2014) "Thermoba-Raman-try":Calibration of spectroscopic barometers and thermometers for mineral inclusions. Earth and Planetary Science Letters, 388, 187-196.

Kouketsu, Y., Nishiyama, T., Ikeda, T., and Enami, M. (2014) Evaluation of residual pressure in an inclusion–host system using negative frequency shift of quartz Raman spectra. American Mineralogist, 99, 433-442.

Nestola, F., Nimis, P., Ziberna, L., Longo, M., Marzoli, A., Harris, J.W., Manghnani, M.H., and Fedortchouk, Y. (2011) First crystal-structure determination of olivine in diamond: Composition and implications for provenance in the Earth's mantle. Earth and Planetary Science Letters, 305, 249-255.

Parkinson, C.D. (2000) Coesite inclusions and prograde compositional zonation of garnet in whiteschist of the HP-UHPM Kokchetav massif, Kazakhstan: a record of progressive UHP metamorphism. Lithos, 52, 215-233.

Rosenfeld, J.L., and Chase, A.B. (1961) Pressure and temperature of crystallization from elastic effects around solid inclusion minerals? American Journal of Science, 259, 519-541.

Sinogeikin, S.V., and Bass, J.D. (2000) Single-crystal elasticity of pyrope and MgO to 20 GPa by Brillouin scattering in the diamond cell. Physics of the Earth and Planetary Interiors, 120, 43-62.

Torquato, S. (2002) Random Heterogeneous Materials: Microstructure and Macroscopic Properties. Springer-Verlag, New York

Zhang, Y. (1998) Mechanical and phase equilibria in inclusion–host systems. Earth and Planetary Science Letters, 157, 209-222.

Always consult and cite the final, published document. See http://www.minsocam.org or GeoscienceWorld

Figure Captions

Figure 1: Sketches of the radial stress against radius in an ideal host-inclusion system. (a) At entrapment (P_{trap}), and at any other point on the isomeke (e.g. at P_{foot} and T_{end}), there is no stress gradient. (b) In the virtual state after decompression of the host to ambient pressure ($=P_{H,end}$), the inclusion is under a radial stress P_I^*. There is therefore a step in stress at the inclusion/host boundary. (c) As a consequence, the inclusion expands until the internal stress drops to $P_{I,end}$ and a stress gradient is developed in the host.

Figure 2: The use of the isomeke concept to calculate residual pressures on an inclusion initially entrapped at P_{trap}**,** T_{trap}**.** (a) The calculation first considers cooling along the isomeke to the final temperature T_{end} where the stress in both the inclusion and the host is uniform and equal to the external pressure, P_{foot}. (b) When the external pressure is reduced (isothermally) to $P_{H,end}$, the un-relaxed inclusion pressure would be P_I^*. Mutual elastic relaxation of host and inclusion then drops the pressure in the inclusion to the final $P_{I,end}$.

Figure 3: A pressure-temperature plot for a quartz inclusion in a garnet. The light lines are the isomekes for alpha-quartz in garnet. The heavy line is the estimated pro-grade path for the Kulet whiteschist (Parkinson 2000). A quartz inclusion entrapped at 0.7 GPa and 380°C lies on an isomeke with P_{foot} = 0.76 GPa. When the garnet is at room conditions, $P_I^* = 0.59\,\mathrm{GPa}$ and the residual pressure is $P_{I,end}$ = 0.44 GPa. At peak metamorphic conditions (T =780°C), the isomeke pressure is 0.52 GPa, and the quartz will be under a pressure of 1.72 GPa, as indicated on the right-hand side of the diagram. Isomekes were calculated with EosFit7c

Always consult and cite the final, published document. See http://www.minsocam.org or GeoscienceWorld

(Angel et al. 2014) from Birch-Murnaghan EoS in combination with a thermal-pressure model (Holland and Powell 2011). The parameters for alpha-quartz: K_0 = 37.12 GPa, $K_0' = 5.99$ (Angel et al. 1997), α_0 = 3.419 x 10^{-5} K^{-1}, θ_E = 314 K. For garnet: K_0 = 174.7 GPa, $K_0' = 5.3$, α_0 = 2.748 x 10^{-5} K^{-1}, θ_E = 757 K.

Always consult and cite the final, published document. See http://www.minsocam.org or GeoscienceWorld

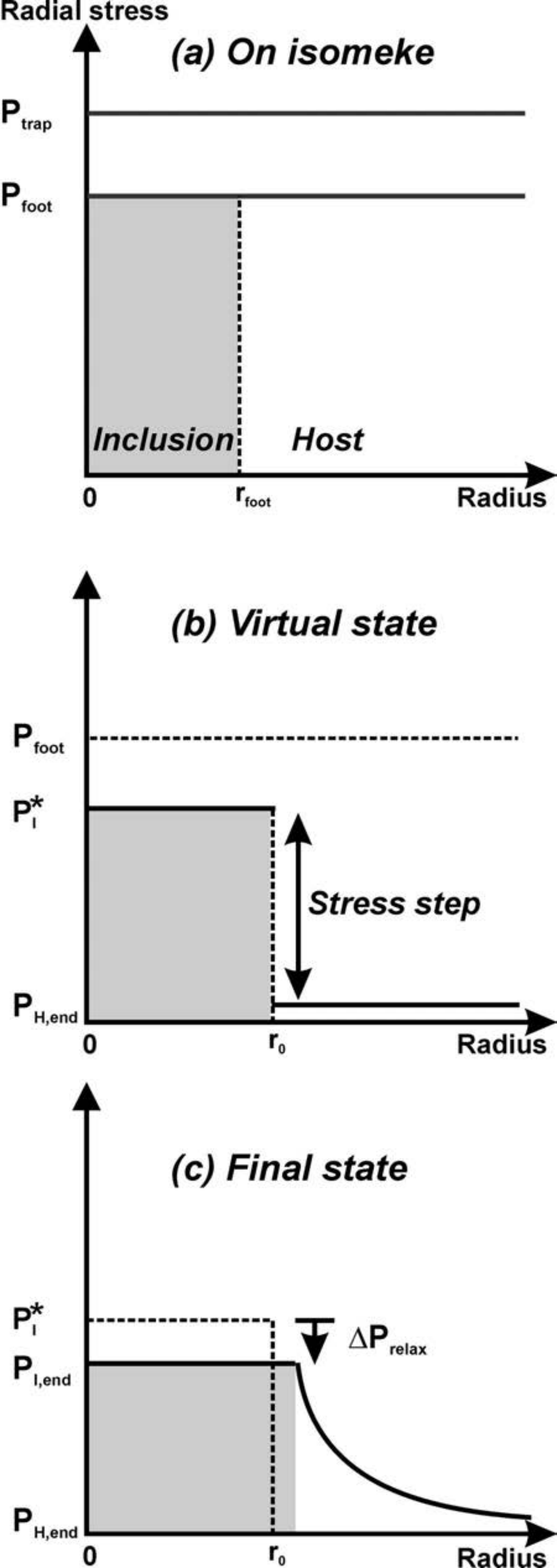
Radial stress
(a) On isomeke
P trap
P foot
Inclusion
Host
0
r foot
Radius
(b) Virtual state
P foot
P*I
Stress step
P H,end
0
r0
Radius
(c) Final state
P*I
ΔP relax
P I,end
P H,end
0
r0
Radius

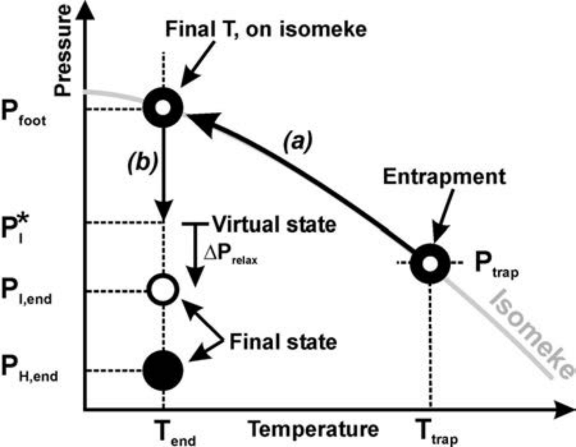

Pressure
Final T, on isomeke
P_foot
(a)
(b)
Entrapment
P*_l
Virtual state
ΔP_relax
P_trap
P_l,end
Isomeke
Final state
P_H,end
T_end
Temperature
T_trap

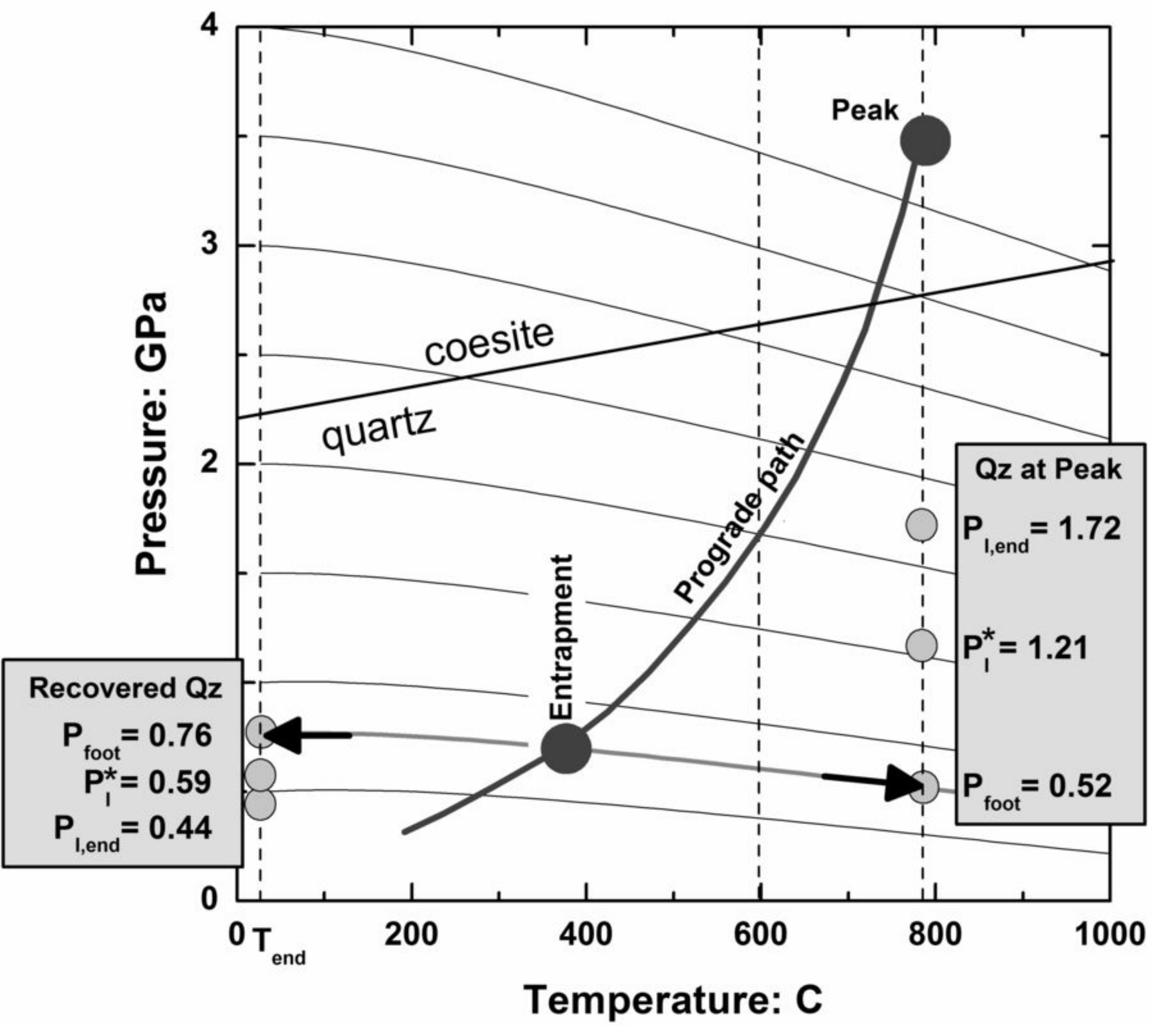

Pressure: GPa
4
3
2
0
Peak
coesite
quartz
Prograde path
Entrapment
Qz at Peak
$P_{I,end}$ = 1.72
P_I^* = 1.21
P_{foot} = 0.52
Recovered Qz
P_{foot} = 0.76
P_I^* = 0.59
$P_{I,end}$ = 0.44
0
T_{end}
200
400
600
800
1000
Temperature: C